WADC TECHNICAL REPORT 53-523 SECURITY INFORMATION

THE EFFECT OF TIP REMOVAL ON THE NATURAL VIBRATIONS OF UNIFORM CANTILEVERED TRIANGULAR PLATES

P. N. Gustafson, W. F. Stokey, C. F. Zorowski

Carnegie Institute of Technology

December 1953

WRIGHT AIR DEVELOPMENT CENTER

WADC Technical Report 53-523

Security Information

THE EFFECT OF TIP REMOVAL ON THE NATURAL VIBRATIONS OF UNIFORM CANTILEVERED TRIANGULAR PLATES

P. N. Gustafson, W. F. Stokey, C. F. Zorowski

Carnegie Institute of Technology

December 1953

Aeronautical Research Laboratory

Contract No. AF 33(616)-294
S2 (54-472)

E. O. No. R471-411
R471-424
R471-408

Project No. 54-610-186

Wright Air Development Center

Air Research and Development Command

United States Air Force

Wright-Patterson Air Force Base, Ohio

ABSTRACT

Experimental results are obtained for the lowest six natural frequencies and the associated nodal lines of trapezoidal plates of uniform thickness clamped on one edge. Three series of plates are investigated. Each series consists of six plates and is developed from a triangular plate by progressively cutting off portions of its tip parallel to its clamped edge, giving a clipped wing effect. Two of the series originate from triangular plates of delta wing plan form with aspect ratios of 2 and 4. A triangular plate with a mean chordline sweepback angle of 45° is used as the basis for the third series. Results are presented in the form of graphs, tables, and photographs. A method of treating plates of non-isotropic material is described. The use of interpolation to extend the results to a broader field of plate shapes is also discussed.

PUBLICATION REVIEW

FOR THE COMMANDER:

NOMENCLATURE

The following nomenclature is used in this paper:

C = root chord (in.)

ℓ_o = half span of complete triangular plate (in.)

$\Delta \ell$ = amount of half span cut from tip (in.)

f = natural frequency (c.p.s.)

f_o = natural frequency of a complete triangular plate (c.p.s.)

$\omega = 2\pi f$ = natural angular frequency (1/sec.)

$\omega_o = 2\pi f_o$

ω_D = dimensionless angular frequency

h = plate thickness (in.)

E = modulus of elasticity ($lb./in^2$)

ρ = mass density of plate material ($\frac{lb.\ sec^2}{in.^4}$)

μ = Poisson's ratio

D = flexural rigidity = $Eh^3/12(1-\mu^2)$

a = scale factor

INTRODUCTION

As an extension to the experimental investigations that have been made of the natural vibrations of cantilevered trinagular plates[1] this study was undertaken to explore the effect of cutting off portions of a triangular plate parallel to its clamped edge. The vibrational characteristics of the trapezoidal plates formed by such cuts appear to be of as much importance as those of triangular plates, since uniform flat plates of both plan-forms approximate basic wing and tail surfaces on many guided missiles and some high speed aircraft.

The variations in plan form of trapezoidal plates are seemingly endless. Yet, if one is willing to confine attention to the case of parallel root and tip chords, any shape may be regarded as a function of three convenient parameters: aspect ratio of the plate (extended to form a complete triangle), sweepback angle of the mean chord line, and ratio of the span removed from the triangle to the original span of the triangle. If, for any values assigned to two of these parameters, it were desired to examine five different cases of the remaining parameter, then 125 plate shapes would be required. Such a program while not impractical, seems overly-ambitious as long as the application of flat plate vibrations to aircraft and missiles is still in an exploratory stage, and while considerable attention is being given to finding analytical solutions.

This report covers eighteen trapezoidal shapes derived from only three triangles. In a later section it will be shown how interpolation may be used to cover the field of delta wing shapes from aspect ratio 2 to aspect ratio 4, and for an aspect ratio of 4, interpolation may again be used to explore mean chord sweepback angles ranging from $\tan^{-1} 0.5$ to $\tan^{-1} 1.0$.

The configurations and designations for the three series of plates investigated are given in Figs. 1, 2, 3, and 4. Series I and II are both developed from triangular plates of the delta wing shape (the trailing edge is a straight line from wing tip to wing tip). The root chord in series I is equal to the total span while in series

II it is half of the total span. Series III originates from a sweptback triangular plate with a root chord equal to half its span and a mean-chord sweepback angle of 45°. The parameter $\Delta l/l_o$ (see Fig. 1) varies over the same range for each series, from 0 to 0.4. All three triangular plates from which the three series are developed have been investigated previously.[1]

The test procedure and equipment used for the experimental determination of the natural frequencies and node lines was the same as that described in reference (1). The plates for each series were cut progressively from the steel plates A-1, A-2, and S-5 used in the authors' earlier investigations of triangular plates. Thus the material properties were kept fixed for a given series. These properties are listed in Table II.

DISCUSSION OF RESULTS

Series I

Figure 5 shows the photographs of the node lines for the first six natural modes of plates I-1, I-2, I-4, and I-6 arranged in order of increasing frequency from left to right. For comparison the node lines for the first six natural modes of the triangular plate from which the series was developed are also shown under the plate designation I-0. The frequencies corresponding to these modes for all five plates shown, as well as those not shown, are given in cycles/sec. and in a dimensionless form in Table I. A discussion of the material properties used in computing these dimensionless frequencies will follow in a subsequent section.

By choosing a given mode in Fig. 5 and observing the behavior of the node lines as the parameter $\Delta l/l_o$ increases, it can be seen that the changes in mode shape from plate to plate follow definite patterns, thus establishing a type of shape family. An exception to this case in series I occurs in the 3rd modes of plates I-0 and I-1 which belong to the shape family represented by the 4th modes of plates I-2, I-4, and I-6 and the 4th modes of plates I-0 and I-1 which belong to the same family as the third modes of I-2, I-4, and I-6. In each mode the frequency increases as more of the tip is removed. This behavior is true for the other two series also and is to be expected, since an increase in $\Delta l/l_o$ brings about a decrease in the mass of the plate. The fundamental mode of all five plates can be generally classified as a spanwise bending mode since only a little bending occurs in the chordwise direction. Similarly, the second mode can be classified roughly as a torsional mode, again remembering that some spanwise bending does occur. It is of little use to attempt a simple classification of the remaining modes since they are composed of varying amounts of chordwise and spanwise bending.

A clear picture of how the amount cut from the tip affects the frequency of the resulting plate is given by the graphs of Fig. 8. Here percentage change in frequency,

$\frac{\omega - \omega_o}{\omega_o}$, is plotted against the parameter $\Delta l/l_o$ for all six modes of all six plates. Each curve corresponds to a given shape family so that the percentage increase in frequency is based on that mode from which the computed mode evolved. Families A, B, E, and F are composed of the 1st, 2nd, 5th, and 6th modes, respectively, of all six plates. Family C consists of the 3rd modes of plates I-0 and I-1 and the 4th modes of I-2, I-4, and I-6 while the 4th modes of I-0 and I-1 along with the 3rd modes of I-2, I-4, and I-6 make up family D.

The curves show that for a given increase in $\Delta l/l_o$ there is a greater percentage increase in frequency in families A and C than in any other family. The fact that family A is primarily a spanwise bending mode and family C has a large percentage of spanwise bending in it while the remaining four families lean heavily toward torsional modes suggests that removing portions of the tip has a greater effect on the frequency of spanwise bending modes than it has on chordwise bending, or "torsional" modes. This can be explained by the fact that the spanwise stiffness increases rapidly as the effective span is decreased while the torsional stiffness is affected only slightly by these changes.

Series II

The node lines for the first six modes of plates II-1, II-2, II-4, and II-6 along with those of II-0 representing the triangular plate from which series II is developed are given in Fig. 6, arranged again in order of increasing frequency from left to right. The frequencies for all modes of all plates in series II including II-0 are given in Table I. It can be seen from the photographs that for this series each given mode makes up a distinct shape family. A general classification can be extended to three modes of this series. The fundamental and third mode are primarily spanwise bending modes while the second mode is quite clearly a torsional mode.

The graphs of Fig. 9 show how the frequencies of the plates of this series are affected by tip removal. The increased effect on bending modes is again shown by

the behavior of the curves of the shape families A and C which correspond to the first and third modes. For $\Delta l/l_o$ in the range 0 to 0.2 curve E behaves much like A and B. A check of the node lines of the fifth mode in this range shows that the mode consists of a large percentage of spanwise bending. From 0.2 to 0.4 curve E behaves much more like B which represents the second mode. A study of the node lines of the fifth mode of plates II-4 and II-6 bears this out as it shows that a considerable amount of torsion is present along with the bending.

Series III

The node lines of series III are presented in the photographs of Fig. 7 arranged in the same manner as the first two series. Table I and the graphs of Fig. 10 show the effect of tip removal on the frequency of vibration. Again in this series all modes of a given order belong to the same shape family. The same general classifications can be applied to the first and second modes of this series that have been given the corresponding modes of the preceeding series. The other modes are too complicated to be given simple classifications. This is borne out by the absence in Fig. 10 of the distinct difference in behavior between bending and torsional and combined modes so apparent in Figs. 8 and 9. However, curve C in Fig. 10 does seem to indicate that the third mode might behave as a bending mode even though it may not appear so from its node lines.

FREQUENCIES OF PLATES OF SIMILAR PLANFORM

The frequencies given in Table I can be used to predict the frequency of a plate with a similar planform but having different size, thickness and material properties by using Eq. (1) in which the primed quantities refer to the plate whose frequency is to be predicted and the unprimed quantities refer to the plate whose frequency is known.[1]

$$f' = \frac{1}{\alpha^2} \frac{h'}{h} \left[\frac{E'}{E} \frac{\rho}{\rho'} \frac{(1-\mu^2)}{(1-\mu'^2)} \right]^{\frac{1}{2}} f \qquad (1)$$

α is a scale factor relating all the dimensions of the two plates except the thickness. It is shown in the development of this expression in reference (1) that this conversion formula is exact only for plates having the same Poisson's ratio but it also provides a good approximation for plates whose Poisson's ratios are not much different.

The use of Equation (1) is made less cumbersome by rearranging it and combining the quantities relating to the plate of known frequency into a dimensionless frequency. Introducing $c' = \alpha c$ into (1) gives

$$f' = \frac{c^2}{c'^2} \frac{h'}{h} \left[\frac{E'}{E} \frac{\rho}{\rho'} \frac{(1-\mu^2)}{(1-\mu'^2)} \right]^{\frac{1}{2}} f \qquad (2)$$

or
$$f' = \frac{h'}{c'^2} \left[\frac{E'}{\rho'(1-\mu'^2)} \right]^{\frac{1}{2}} \left\{ \frac{c^2}{h} \left[\frac{\rho(1-\mu^2)}{E} \right]^{\frac{1}{2}} f \right\} \qquad (3)$$

but
$$\frac{c^2}{h} \left[\frac{\rho(1-\mu^2)}{E} \right]^{\frac{1}{2}} f = \frac{1}{2\pi\sqrt{12}} \frac{\omega}{\sqrt{D/\rho h c^4}} \qquad (4)$$

Where $\omega = 2\pi f$, $D = \dfrac{E h^3}{12(1-\mu^2)}$

Therefore (3) can be written as

$$\omega' = \omega_D \sqrt{\frac{D'}{\rho' h' c'^4}} \qquad (5)$$

where
$$\omega_D = \frac{\omega}{\sqrt{D/\rho h c^4}} \quad = \text{dimensionless frequency} \qquad (6)$$

This form of the frequency is used in reference (3).

Equation (5) gives the unknown frequency of the new plate in terms of its properties and dimensions and the dimensionless frequency, ω_D . It is seen that once ω_D is computed, the user of this transformation need no longer be concerned with the properties and dimensions of the original plate for which the frequency is known. This development also eliminates the scale factor α and introduces in its place a significant dimension of the plate, the root chord. The dimensionless frequencies tabulated in Table I were computed from Eq. (6).

FREQUENCIES OF PLATES OF DIFFERENT PLANFORM

The graphs and tables of this report may be used to estimate the natural frequencies of a plate having a planform within the range, or slightly outside the range, of the planforms actually tested. This may be done by a simple interpolation or extrapolation. Confidence may be placed in such a procedure as long as the numerical values being interpolated between, or extrapolated from, are not far apart. A study of the effects of aspect ratio and sweepback on triangular plates[1] should also prove helpful in determining whether the frequency behavior is sufficiently linear in the interval being considered. The method will be demonstrated by several examples.

I. Interpolation applied to plate of truncated delta-wing planform.

In Fig. 11(a) is shown a delta-wing planform which is intermediate in shape between the plates of Series I and Series II. The aspect ratios of the complete triangular delta-wing shapes are as follows:

Series I. Aspect Ratio = $\frac{2L}{C} = \frac{2(20)}{20} = 2$

Series II. Aspect Ratio = $\frac{2L}{C} = \frac{2(20)}{10} = 4$

Plate (a) Aspect Ratio = $\frac{2L}{C} = \frac{2(20)}{16} = 2.5$

The graphs of frequency vs. aspect ratio for complete triangular plates[1] reveal that in the range from 2 to 4 the frequency of the first six natural modes are approximately

TABLE I

MEASURED AND DIMENSIONLESS FREQUENCIES FOR TIP REMOVALS OF FROM 0 TO 40 PERCENT OF SPAN

SERIES I

Family	A		B		C		D		E		F	
Mode	1		2		3		4		5		6	
$\Delta\ell/\ell_o$	f	ω_D	f	ω_D	f	ω_D	f	ω_D	f	ω_D	f	ω_D
0	32.8	22.0	91	58.7	164	110	181	119	283	186	348	228
.1	34	22.7	93	60.0	179	120	181	119	293	192	352	231
.2	38.5	25.8	97.6	63.0	184*	121	212**	142	302	198	362	238
.25	41.9	28.0	99.4	64.1	186*	122	235**	157	304	200	366	240
.3	48.3	32.3	103.4	66.8	190*	125	266**	178	308	202	379	249
.35	53.7	35.9	107.4	69.4	196*	129	299**	200	314	206	404	265
.4	60	40.1	112	72.3	202*	133	350**	234	312	205	436	286

* Family D
** Family C

SERIES II

Family	A		B		C		D		E		F	
Mode	1		2		3		4		5		6	
$\Delta\ell/\ell_o$	f	ω_D	f	ω_D	f	ω_D	f	ω_D	f	ω_D	f	ω_D
0	34.5	5.87	136	23.8	190	32.4	325	56.1	441	76.0	578	99.7
.1	37	6.30	142	24.8	198	33.7	335	57.8	482	83.1	583	101
.2	42	7.15	153	26.7	223	38.0	364	62.8	561	96.9	598	103
.25	46	7.83	157	27.4	243	41.4	374	64.5	596	103	621	107
.3	50.5	8.60	161	28.2	268	45.6	385	66.5	606	105	660	114
.35	56	9.53	169	29.5	300	51.1	410	70.8	629	109	695	120
.4	64	10.9	175	30.6	339	57.7	434	74.9	639	110	718	124

TABLE I (cont.)

SERIES III

Family	A		B		C		D		E		F	
Mode	1		2		3		4		5		6	
$\Delta\ell/\ell_o$	f	ω_D	f	ω_D	f	ω_D	f	ω_D	f	ω_D	f	ω_D
0	26.3	4.50	101	17.6	171	29.3	259	44.7	346	59.7	522	90.0
.1	27.9	4.78	110	19.2	184	31.5	274	47.3	376	64.9	525	90.5
.2	31.5	5.39	122	21.3	198	33.9	289	49.8	438	75.6	542	93.5
.25	34.8	5.96	130	22.7	215	36.8	300	51.7	476	82.1	567	97.8
.3	38.5	6.59	136	23.8	243	41.6	312	53.8	505	87.1	623	107
.35	44.9	7.69	143	25.0	277	47.4	327	56.4	540	93.2	674	116
.4	51.7	8.85	151	26.4	314	53.8	347	59.9	573	98.9	699	121

TABLE II

Plate Properties

Property / Plate	Experimentally Determined				μ (assumed)
	Spanwise E ($\#/in.^2$)	Chordwise E ($\#/in.^2$)	ρ_g ($\#/in.^3$)	h (in.)	
Series - I	29.3×10^6	31.5×10^6	.281	.0622	.29
Series - II	29.2×10^6	27.8×10^6	.281	.0613	.29
Series - III	29.0×10^6	27.8×10^6	.281	.0613	.29
10" x 10" square	29.3×10^6	31.5×10^6	.282	.0627	.29
18" x $2\frac{1}{2}$" beam	29.8×10^6	_____	.282	.0585	.29

linear functions of aspect ratio and it was decided to use this as a basis for interpolation in the truncated plates as well.

Furthermore it has been found that interpolation produced better results, on the whole, when the semi-span of the complete delta plate was used to compute dimensionless frequencies, rather than the chord. Noting from Eq. (6) that the dimensionless frequency varies as the square of the length, c, then the dimensionless frequencies of Table I, Series I should be divided by 4 if the 10" semi-span were used to compute ω_D. Series II dimensionless frequencies would be unaffected since the semi-span and chord are equal. Table III gives the dimensionless frequencies for the complete triangular plate ($\Delta\ell/\ell_o=0$) of Series I.

TABLE III

Dimensionless Frequencies for Series I, Based on Span

Mode	1	2	3	4	5	6
ω_D for $\Delta\ell/\ell_o = 0$	5.50	14.7	27.5	29.8	46.5	57.0

For a numerical example, consider the second mode of vibration (Family B) of the plate shape in Fig. 11 (a). $\Delta\ell/\ell_o = \frac{3.8}{10} = 0.38$

From the graph of family B, Series I, Fig. 8, the frequency ratio is $\Delta\omega/\omega_o = 0.22$

From the graph of family B, Series II, Fig. 9, the frequency ratio is $\Delta\omega/\omega_o = 0.27$

Then ω_D for Series I is $1.22 \times 58.7/4 = 17.9$ and ω_D for Series II is $1.27 \times 23.8 = 30.2$.

Interpolating, we obtain ω_D for plate (a) $= 17.9 + \frac{0.5}{2.0}(12.3) = 21.0$

Next the frequency of an actual steel plate is predicted, assuming the elastic properties as given below.

$h = 0.059$ in.

$E = 29 \times 10^6$ psi

$\mu = 0.29$

$D = \frac{Eh^3}{12(1-\mu^2)} = 560$ lb.-in.

$(\ell/2)^4 = 10^4$ in^4

$\rho = \frac{0.282}{386} = 7.31 \times 10^{-4} \frac{\text{lb.-sec}^2}{\text{in}^4}$

Then $\omega = \omega_0 \sqrt{\frac{D}{\rho h (\frac{l}{2})^4}} = 35.4\,\omega_0$ (7)

Thus for the second mode of this plate, $f = \frac{35.4 \times 21.0}{2\pi} = 118$ cycles per second. The experimentally measured frequency of this plate was 116 cycles per second.

By this procedure of interpolating between Series I and II to find ω_0, and then using Eq. (7), the first six natural frequencies of this plate were calculated and are compared with experimental results in Table IV.

TABLE IV

Comparison of interpolation with experimentally observed frequency, Plate (a)

Mode Family	A	B	D	C	E	F
Mode Number	1	2	3	4	5	6
Predicted Frequency	55	118	241	308	372	465
Measured Frequency	52.2	116	225	308	370	447
Percent Difference	+5.4	+1.7	+7.1	0	+0.5	+4.0

2. Interpolation applied to plate of truncated, sweptback planform.

In Fig. 11 (b) is shown a plate which is intermediate in shape between the plates of Series II and Series III. The completed triangular wing has a total span of 20" and root chord of 10" as do the plates of Series II and III, so that all three plates have the same aspect ratio. The graphs of frequency vs. tangent of sweepback angle for complete triangular plates[1] reveal that in the range from 0.5 to 1.0 the frequencies of the first six natural modes are approximately linear functions of the tangent of the sweepback angle (based on mean chord line) and it was decided to use this as a basis for interpolation in the truncated plates as well.

As an example, consider the third mode of plate (b) in Fig. 11.

$$\Delta l / l_0 = \frac{3.25}{10} = 0.325$$

From the graph of family C, Series II, Fig. 9, the frequency ratio is $\Delta\omega/\omega_o = 0.49$

From the graph of family C, Series III, Fig. 10, the frequency ratio is $\Delta\omega/\omega_o = 0.51$

Then ω_D for Series II is $1.49 \times 32.4 = 48.2$

and ω_D for Series III is $1.51 \times 29.3 = 44.2$

Furthermore the sweepback tangents are

Series I, $\tan\alpha = 0.5$

Series II, $\tan\alpha = 1.0$

Plate (b), $\tan\alpha = 0.7$

Then ω_D for plate (b) $= 48.2 - \frac{0.2}{0.5} \times 4.0 = 46.6$

Next the frequency of an actual steel plate is predicted assuming the elastic properties as given below. The modulus of elasticity is based on experiments made on plates of similar steel.

$h = 0.0613$ in.

$E = 28.5 \times 10^6$ psi

$\mu = 0.29$

$D = \frac{Eh^3}{12(1-\mu^2)} = 598$ lb-in

$c^4 = 10^4$ in^4

$\rho = \frac{0.281}{386} = 7.28 \times 10^{-4} \frac{\text{lb.-sec}^2}{\text{in}^4}$

Then $\omega = \omega_D \sqrt{\frac{D}{\rho h c^4}} = 36.6\,\omega_D$ (8)

Thus for the third mode of this plate, $f = \frac{36.6 \times 46.6}{2\pi} = 272$ cycles per second.

The experimentally measured frequency for this plate was 270 cycles per second.

A comparison between predicted and measured frequencies for the first six modes of this plate is given in Table V.

TABLE V

Comparison of interpolation with experimentally observed frequency, Plate (b)

Mode Family	A	B	C	D	E	F
Mode Number	1	2	3	4	5	6
Predicted Frequency	48.2	158	272	366	581	668
Measured Frequency	47.3	150	270	350	579	650
Percent Difference	+ 1.9	+ 5.3	+ 0.7	+ 4.6	+ 0.3	+ 2.8

As a closing remark on interpolation, it seems evident from the photographs of Figs. 5, 6, and 7, that interpolation may be applied to shapes of natural modes, as well as to the frequencies of vibration.

THE EFFECT OF NON-ISOTROPY IN PLATE MATERIAL

It is well known that the rolling process introduces a directional character into the grain structure of metals, the grains being longer in the direction of rolling. This orientation of grains is only partly relieved by annealing. It has been found that the ultimate tensile strength and ductility of steel may vary considerably, depending on the direction in which these properties are measured in relation to the rolled plate.[2] In attempting to check the accuracy of our techniques by comparison with work of Barton[3] and Dalley and Ripperger[4] we began to suspect a difference in the moduli of elasticity in the spanwise and chordwise directions for the steel plate being used. Careful static beam deflection tests revealed that the moduli in the two directions differed by as much as 7 percent, one plate having 29.3×10^6 psi in the direction of rolling and 31.5×10^6 psi perpendicular to the direction of rolling.

In determining the modulus of elasticity, two beam specimens, 1/4 inch wide and 1/2 inch wide, were cut from both the spanwise and chordwise directions for each of the three original triangular plates. The spanwise direction in Series I and

TABLE VI

Comparison of Analytical and Experimental Frequencies for Square Plate and Beam

	10" x 10" Plate				18" x 2½" Beam		
Mode \ ω_D	Author's (experimental) value	Computed value reference (3)	% deviation	Experimental value reference (4)	Author's (experimental) value	Computed value reference (5)	% devia.
1	3.35	3.49	− 4.0	3.37	3.46	3.52	− 1.7.
2	8.53	8.55	− 0.2	8.26	21.54	22.4	− 4.0
3	20.90	21.44	− 2.5	20.55	60.85	61.70	− 1.4
4	26.72	27.46	− 2.7	27.15	119.9	121.0	− 0.9
5	30.61	31.17	− 1.8	29.75	197.5	200.0	− 1.3

the chordwise direction in Series II and III coincided with the direction of rolling. The material was hot rolled steel approximately 1/16" thick. The edges of the beams were accurately ground to give a constant uniform cross section throughout. They were then placed on specially constructed knife edges and deflections were measured at the center of a 10-inch span, under the action of centrally applied loads. The load on each beam was gradually increased to a point near the limit of elastic behavior, and then gradually decreased to zero. Curves of load versus deflection were then drawn to insure that the tests were conducted in the range in which deflection and load were linearly related. The modulus of elasticity was then computed from the compiled deflection and load data, using elementary beam theory. No significant difference was found between the moduli given by the 1/4" and 1/2" beams and it may be concluded that specimens of both widths were amenable to simple beam theory.

Table II gives the results of these experiments in the form of an average spanwise and chordwise modulus of elasticity for each plate. Also included in this table are the measured densities of the plate material and the values of Poisson's ratio used in computing the dimensionless frequencies.

The variation of modulus of elasticity with direction in a non-isotropic plates poses the question of what value of E should be used in predicting new frequencies and computing dimensionless frequencies to insure the greatest accuracy. Since bending in a given direction is related to the modulus of elasticity in that same direction it appears that it would be proper when attempting to predict, say, the frequency of a spanwise bending mode to use the spanwise modulus of elasticity. The dimensionless frequency used for this purpose should be given the same consideration if it is obtained from a plate of non-isotropic material. This procedure is quite straightforward for modes consisting primarily of either spanwise or chordwise bending providing the moduli of elasticity of the material are known in

these directions. However, modes in which bending in both directions are combined make it necessary to use some average of the two moduli depending on the mode shape. The spanwise E's were used in computing the dimensionless frequencies of shape families A and C in each series while the chordwise E's were used for shape families B. Due to the complicated shapes contained in families D, E, and F, arithmetic averages of the spanwise and chordwise moduli were used in computing their dimensionless frequencies.

Another effect of non-isotropy should be pointed out. The shape of a natural mode is unquestionably altered from the shape that would exist if the plate were isotropic. We feel that even for appreciably different stiffness in the spanwise and chordwise directions, the effect on modes which are predominantly spanwise or chordwise bending would be quite small. For more complicated modes the effect would be more pronounced, and no doubt some of the node lines in Figs. 5-7 are not quite the same as would be observed for a truly isotropic plate. However, it is unlikely that the 7 percent maximum difference in spanwise and chordwise moduli has introduced serious differences in shape.

CHECK ON ACCURACY OF EXPERIMENTS

In order to establish some idea as to the degree of accuracy of the experimentally determined plate frequencies, and as a check on effectiveness of the clamping, the first five natural frequencies of a 10" x 10" cantilevered square plate and of an 18" x $2\frac{1}{2}$" beam were determined using the same test equipment and procedure used on the trapezoidal plates. A comparison was then made between the observed frequencies and existing experimental and theoretical results. The results of this investigation are presented in Table VI.

Before the dimensionless frequencies were computed, tests were run to determine the moduli of elasticity of the square plate and beam, which were cut from 1/16 inch

commercial cold rolled steel. These tests were conducted in a manner similar to those previously discussed with the exception that only the spanwise modulus was determined for the beam specimen since only spanwise bending occurred in the first five modes. The moduli determined for the square plate and beam are listed with those of the triangular plates in Table II. The first and third modes of the square plate are primarily bending modes, the second and fourth consist chiefly of torsion, and the fifth is a combination of both. Hence in computing the theoretical frequencies the spanwise modulus was used for the bending modes, the chordwise modulus for the torsional modes and an arithmetic average of both was used for the fifth mode.

When the appropriate modulus is used, the dimensionless frequencies obtained for the square plate agree quite well with both the numerical solutions of Barton[3] and the experimental work of Dalley and Ripperger[4].

The measured beam frequencies also agree closely with the theoretical values based on elementary beam theory[5].

REFERENCES

1. Gustafson, P. N., Stokey, W. F., and Zorowski, C. F.,
"An Experimental Study of Natural Vibrations of Cantilevered Triangular Plates."
Journal of the Aeronautical Sciences, Vol. 20, No. 5, May, 1953.

2. Barrett, C. S.,
"Structure of Metals," 2nd. Ed. McGraw-Hill Book Company, Inc. New York, 1952.

3. Barton, M. V.,
"Vibration of Rectangular and Skew Cantilever Plates," Journal of Applied Mechanics,
Vol. 18, No. 2, June, 1951.

4. Dalley, J. W., and Ripperger, E. A.,
"Experimental Values of Natural Frequencies for Skew and Cantilever Rectangular
Plates," Society for Experimental Stress Analysis Proceedings, Vol. 9, No. 2, 1952.

5. Den Hartog, J. P.,
"Mechanical Vibrations," 3rd Ed., McGraw-Hill Book Company, Inc., New York, 1947.

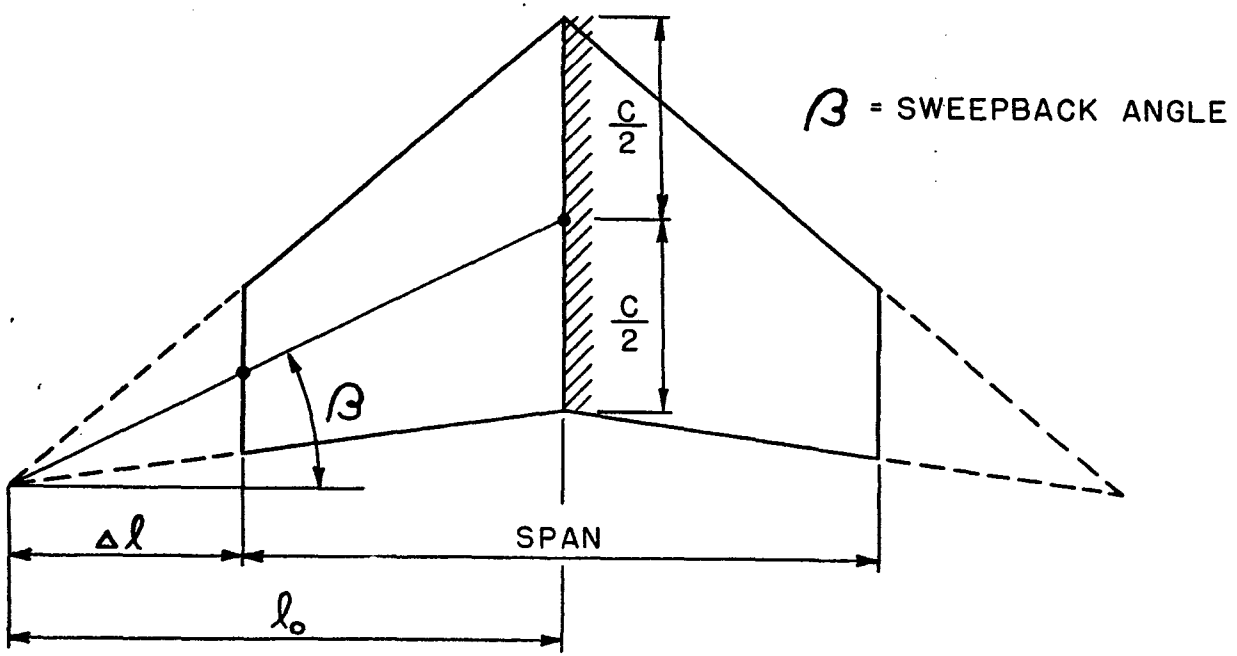

FIG. 1. PLATE NOMENCLATURE

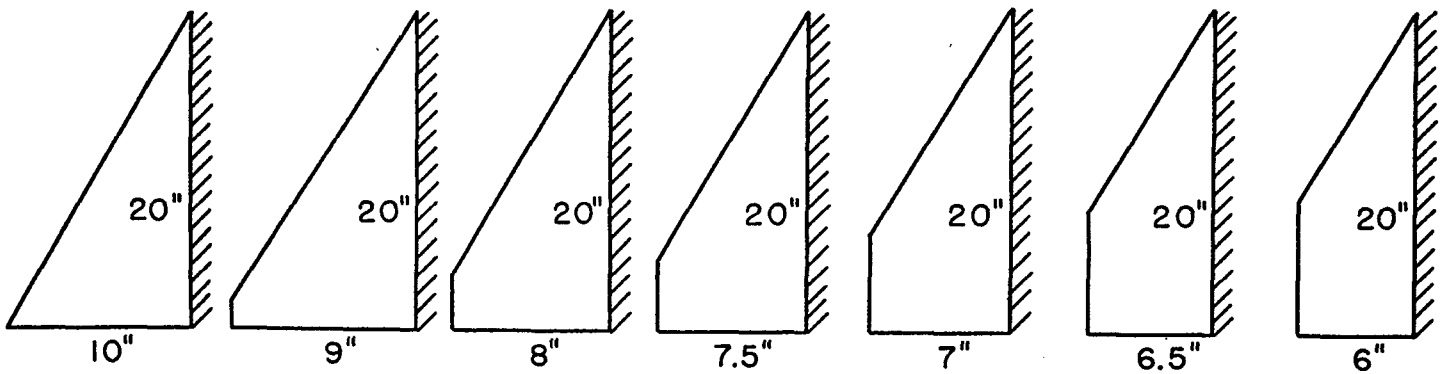

$\frac{\Delta l}{l_o}$	0	.1	.2	.25	.3	.35	.4
DESIGNATION	I-0	I-1	I-2	I-3	I-4	I-5	I-6

FIG. 2. PLATE CONFIGURATIONS FOR SERIES I.

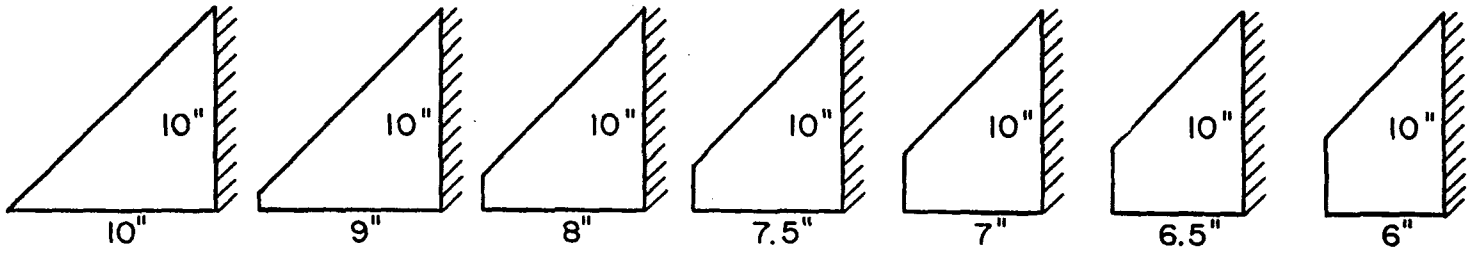

$\frac{\Delta l}{l_o}$	0	.1	.2	.25	.3	.35	.4
DESIGNATION	II-0	II-1	II-2	II-3	II-4	II-5	II-6

FIG. 3. PLATE CONFIGURATIONS FOR SERIES II.

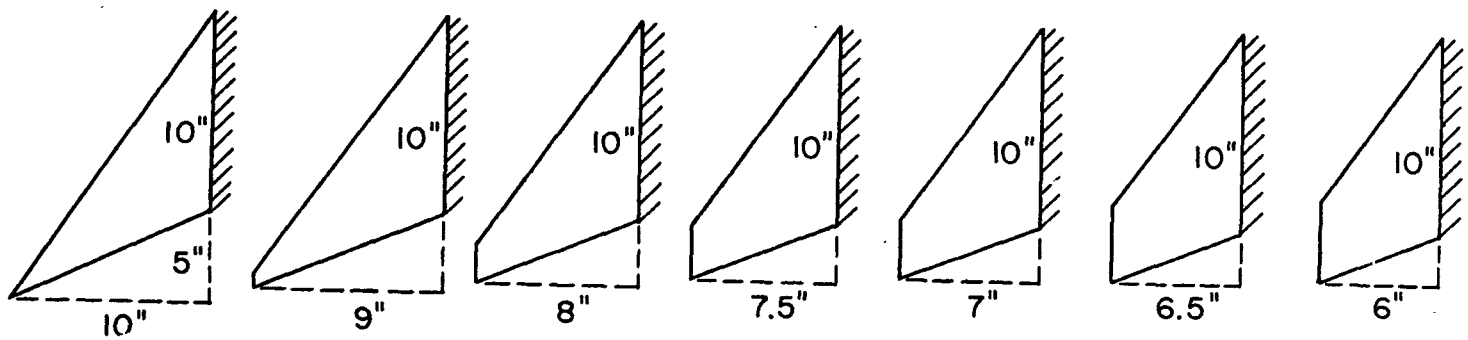

$\frac{\Delta \ell}{\ell_o}$	0	.1	.2	.25	.3	.35	.4
DESIGNATION	III-0	III-1	III-2	III-3	III-4	III-5	III-6

FIG. 4. PLATE CONFIGURATIONS FOR SERIES III.

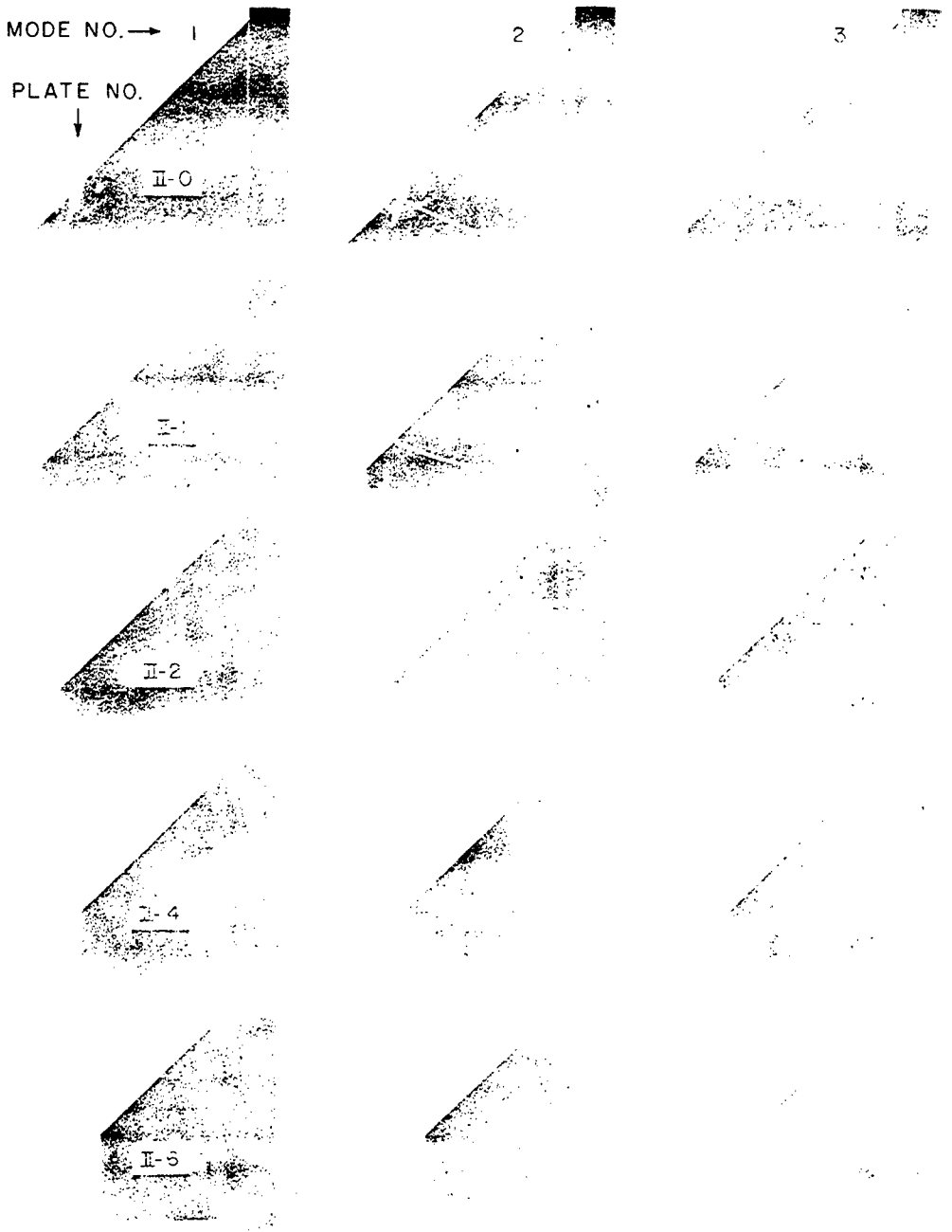

FIG. 6. MODE LINES FOR [illegible] II PLATE.

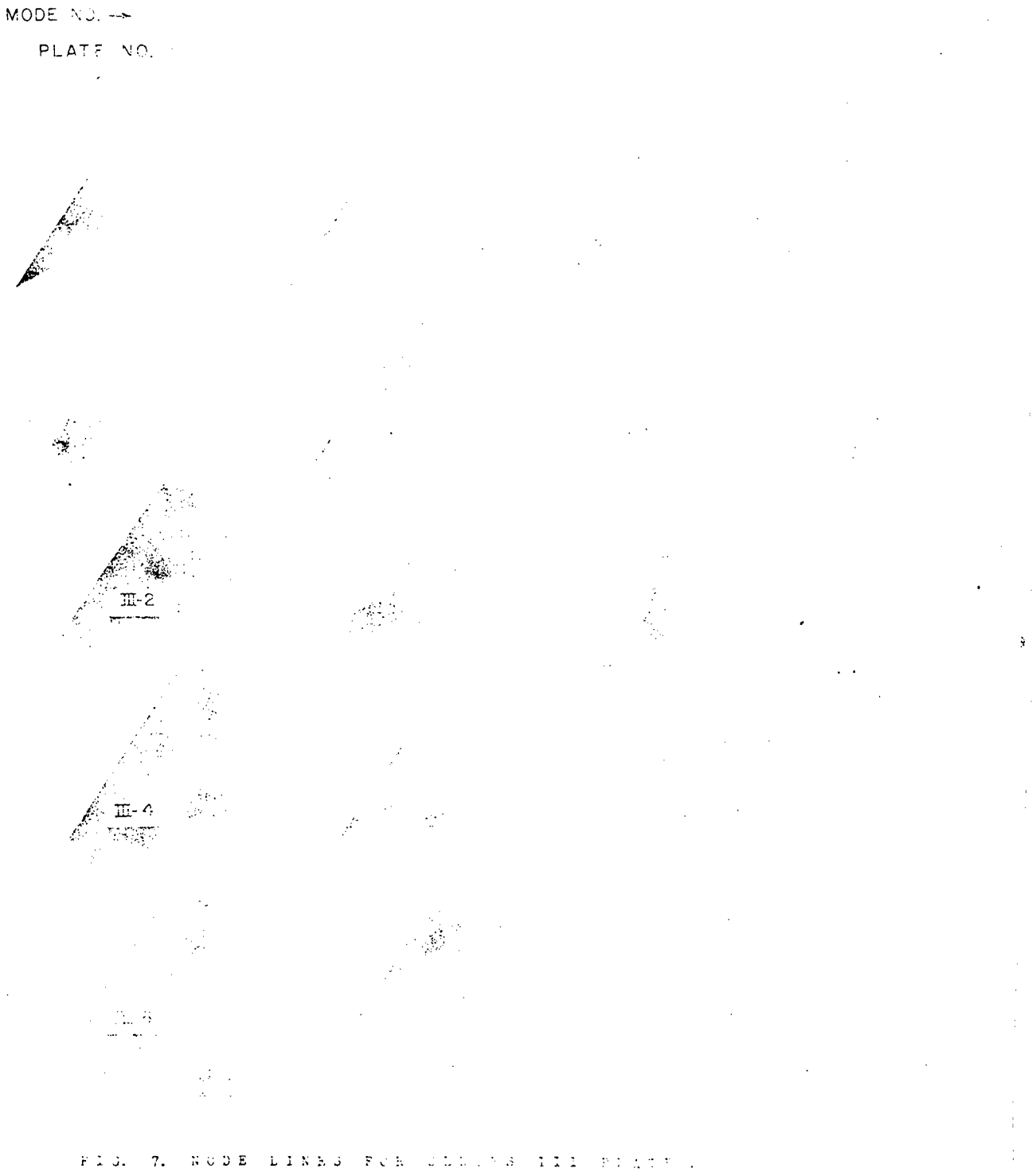

FIG. 7. MODE LINES FOR [illegible] III PLATE.

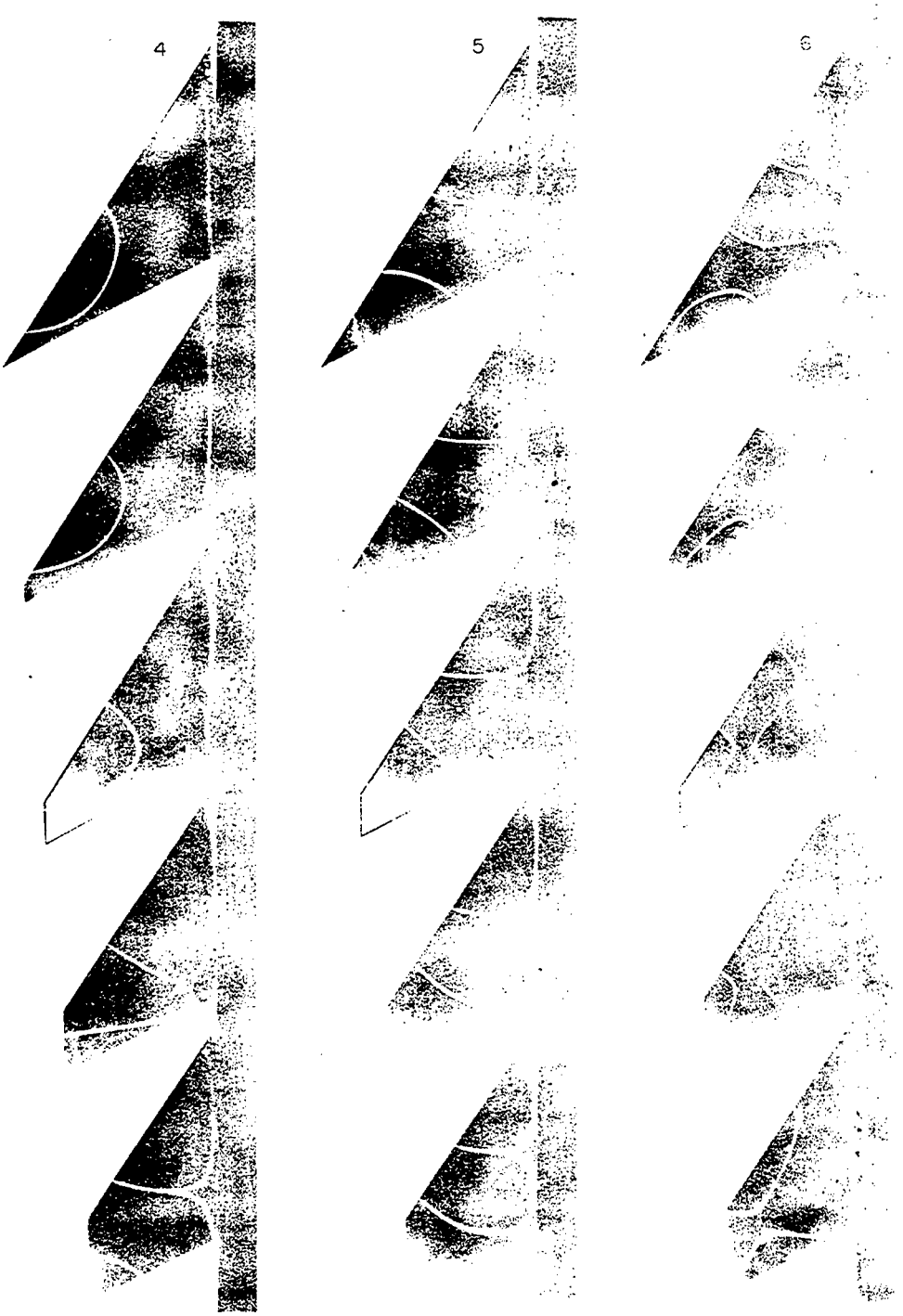

FIG. 7. CONCLUDED

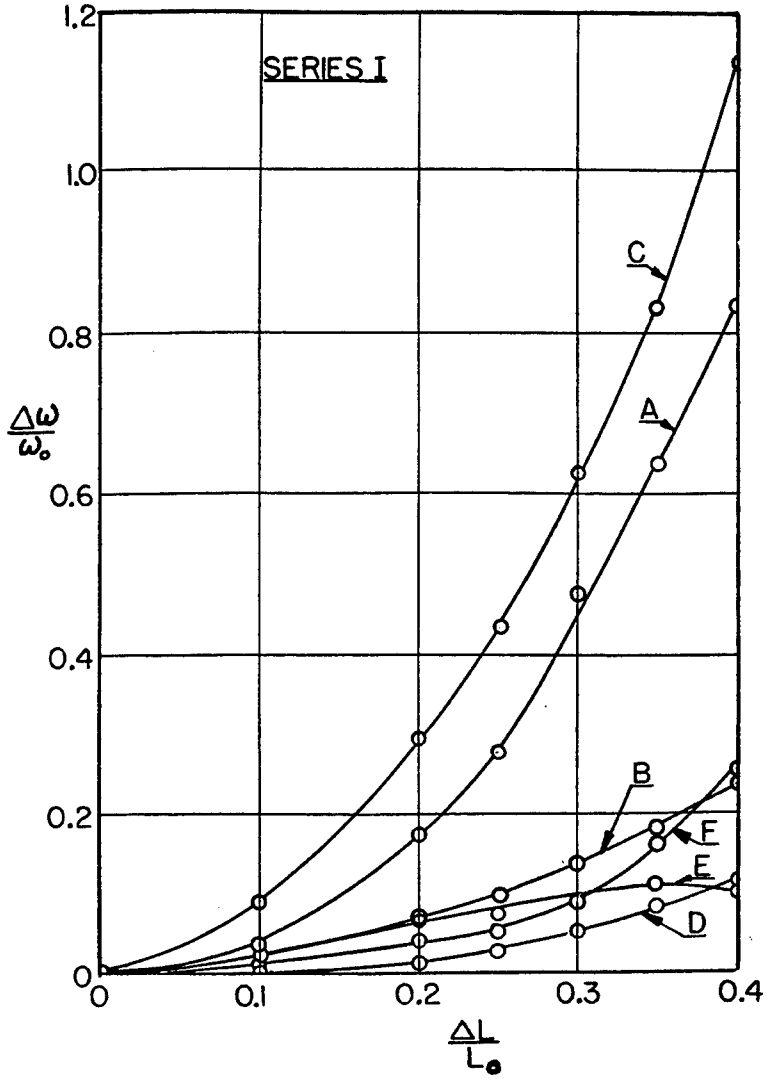

FIG. 8. EFFECT OF TIP REMOVAL ON FREQUENCY, SERIES I.

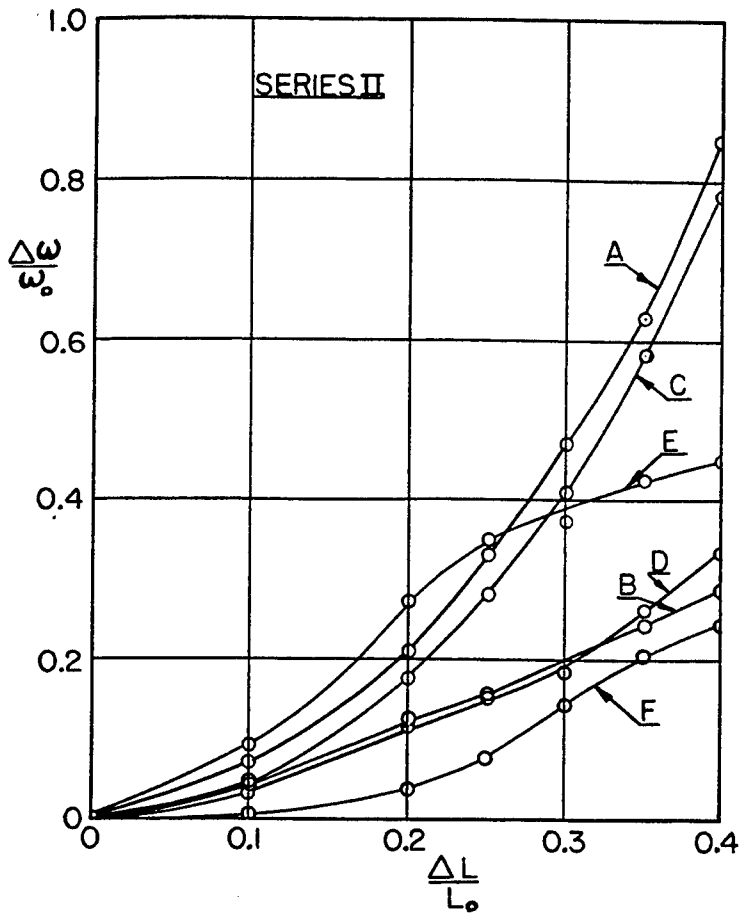

FIG. 9. EFFECT OF TIP REMOVAL ON FREQUENCY, SERIES II.

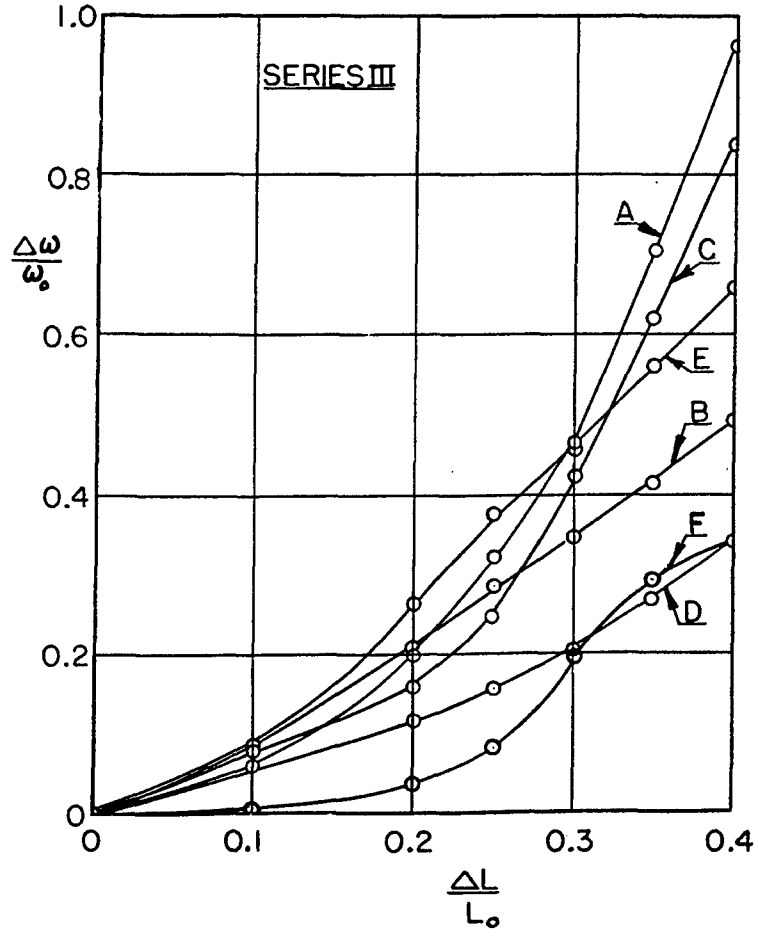

FIG. 10. EFFECT OF TIP REMOVAL ON FREQUENCY, SERIES III

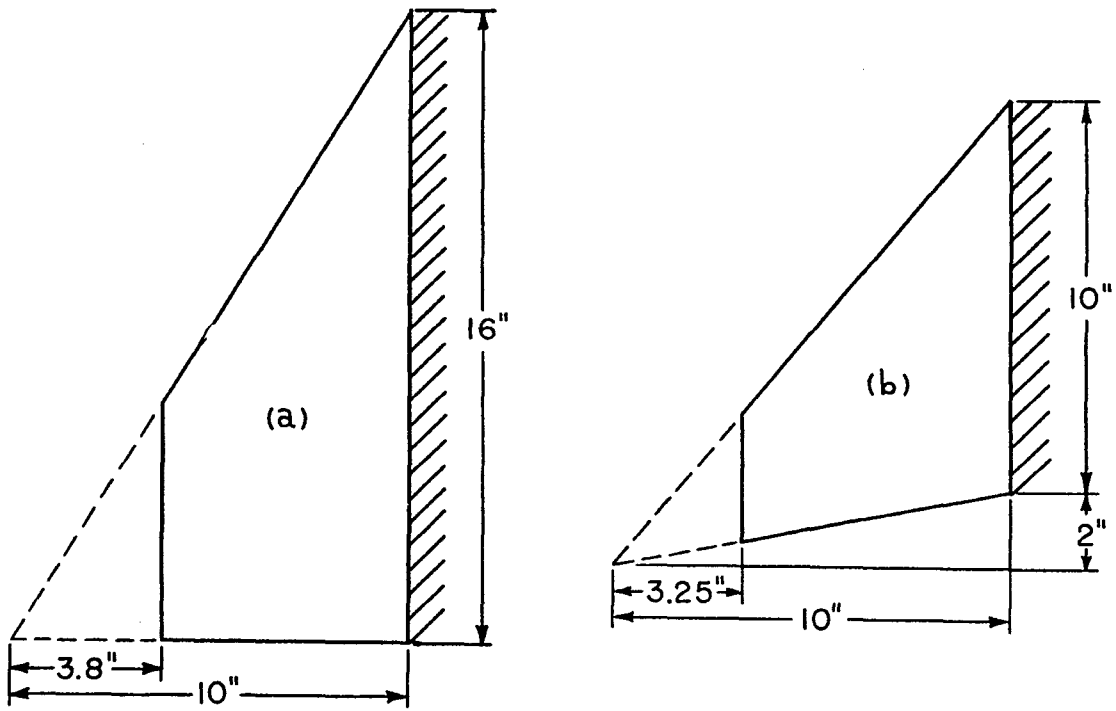

FIG. 11. EXAMPLES OF METHOD OF INTERPOLATION